Geoid
Journal of Geodesy and Geomatics

Geoid Vol. 20, No. 2, 2025, 9-21

P-ISSN: 1858-2281; E-ISSN: 2442-3998

Refining the Indonesian Geoid Model: A Comparative Study of Global Geopotential Models in East Kalimantan

Fahri Dean Alvito[1], Zulfikar Adlan Nadzir*[1], Misfallah Nurhayati[1]
[1]Program Studi Teknik Geomatika, Fakultas Infrastruktur dan Kewilayahan, Institut Teknologi Sumatera, Lampung Selatan, 35365, Indonesia
*Corresponding author: zulfikar.nadzir@gt.itera.ac.id

Received: 11032025; Revised: 29072025; Accepted: 12082025; Published: 05092025

Abstract: Gravity field along with its derivative, geoid, is one of the important pillars of Geodesy. The geoid is utilized in many countries as the vertical reference system, Indonesia as well. However, Indonesia is unique in topography, made the computation of geoid model throughout the archipelago a challenge. The development of geoid model in Indonesia has 4 phases, with the latest in 2020 and 2023. INAGEOID2020 is the Indonesian geoid model used as vertical reference frame for vertical control in Indonesia, updated to version 2.0 in 2023. However, it has not achieved the target accuracy of 5 cm throughout the country. INAGEOID2020 v2.0 is based on the EGM2008 global geopotential model (GGM) with order and degree 360, which is now nearly 20 years old. The implementation of EGM2008 into the regional model also lacked a fitting process, relying solely on functional calculations. This study proposes using modern GGMs, namely EGM2008, XGM2019e, and SGG-UGM-2, along with a fitting process to improve geoid modeling, to optimize the future iteration of Indonesian Geoid Model. The research compares the gravimetric undulations of these models to geometric undulations at 264 validation points, both with and without fitting in East Kalimantan. The fitting improved the accuracy of EGM2008 and XGM2019e, but SGG-UGM-2 performed worse due to elevation discrepancies both before and after the fitting, mainly due to difference on the starting point close to the coast. XGM2019e at degree 2190, truncated to 720 and 360 showed the best results after the fitting, achieving standard deviation and root mean square error (RMSE) values of 0.061 m and 0.064 m, respectively. The performance of EGM2008 is not far behind XGM2019e. This finding indicates that the XGM2019e is the best out the trio, making it a promising alternative to be utilized for future geoid modeling in Indonesia.

Keywords: geoid; GGM; fitting; INAGEOID2020; validation

How to cite: Alvito, F.D., Nadzir, Z.A., & Nurhayati, M. (2025). Refining the Indonesian Geoid Model: A Comparative Study of Global Geopotential Models in East Kalimantan. *Geoid, 20*(2), 9 - 21.

Introduction

In Geodesy, defining gravity field of the Earth is fundamental since it is the second out of three pillar (Vaníček & Krakiwsky, 1995). According to Classical Mechanics, gravity is a resultant of all forces acting on the Earth's surface, namely the gravitational force and centrifugal force (Hofmann-Wellenhof & Moritz, 2006), of which the fundamental difference between gravity and gravitation. Various methods have been developed, utilized and updated for any type of Earth's surface (land, air and water) throughout the years to obtain more accurate and precise gravity field. These methods are, among others, shipborne (Feng et al., 2012), airborne (Sabri et al., 2021) and satellite (Bramanto et al., 2022). One of the derivative parameter from gravity is called Geoid, along with gravity anomaly (Δg), defined as the difference between gravity on geoid surface (g_p) and normal gravity vector on the reference ellipsoid (γ_Q) (Hofmann-Wellenhof et al., 2008). Geoid is a geographical representation of the Earth's shape with respect to the global mean sea level – MSL with all forces that acting on it excluded (Sansò & Sideris, 2013), of which first coined by Gauss in 1828 and measured the first time by Listing in 1871 (Seeber, 2003). It serves as a vertical reference for many countries, including Australia (Featherstone et al., 2012), India (Goyal et al., 2021) and Indonesia. Indonesia herself has 4 phase and iteration of her geoid model, started from 1981 that was solely based on terrestrial data (Kahar, 1982), updated in 1996 which developed from the Indonesian Gravity Database of 1994 (Kahar et al., 1996) and lastly, INAGEOID2020 in 2020 and its second version, the v2.0. INAGEOID2020 was initially published by the Badan Informasi Geospasial (BIG) in Indonesia as a vertical reference for several geospatial applications

(Pahlevi et al., 2024). It was subsequently revised in INAGEOID2020 version 2.0 while acting as a fulfillment of the Decree of the Head of Indonesian Geospatial Agency Number 15 on 2013 (Nadzir & Rahmadhani, 2024). Nevertheless, INAGEOID2020 v2.0 still exhibits deficiencies in terms of precision, particularly in attaining the prescribed 5 cm accuracy objective across Indonesia (Pahlevi & Pramono, 2022).

Indonesia, with its unique condition as the biggest archipelago in the world, has a particular challenge on estimating her geoid. This obstacle mainly stems from the challenge on obtaining accurate and precise gravity over a huge swath of Indonesian seas, as demonstrated on (Nadzir & Rahmadhani, 2024). In order to solve this problem, one could utilize airborne gravity (Udama et al., 2024), altimetry (Andersen & Knudsen, 2019) and global geopotential model (GGM) (Pavlis et al., 2012) to be utilized as the substitute over ocean. INAGEOID2020 itself has undergone multiple assessments and revisions since its inaugural release. INAGEOID2020 v2.0 implemented significant enhancements by incorporating the most recent gravity data from both terrestrial and airborne sources, along with refining data processing and geoid fitting techniques while utilizing EGM2008 and DTU17 as well as SRTM30 topographical model as an additional input. The objective of these refinements is to enhance the precision of the model as a dependable national vertical reference, albeit with slight deficiency as found by previous research that the accuracy level couldn't reach 5 cm, reaching sub-decimeter instead (Lestari et al., 2023).

Global geopotential model itself is a mathematical model that represents the distribution of gravitational potential on Earth, derived from analysis of gravimetric satellite measurements. The primary objective of the global geopotential model is to comprehend the fluctuation of gravity over the Earth's surface, so facilitating several disciplines including geodesy, geophysics, navigation, and deformation measurements. Various data sources build the GGM; altimetry satellite, gravity satellite, gravity survey (terrestrial, shipborne and airborne) and elevation data (DEM – Digital Elevation Model) (Förste et al., 2014; Zingerle et al., 2020). In recent years many GGM have been developed with varying degrees of accuracy based on the methods utilized, e.g., EGM2008, EIGEN-6C4 and XGM2019e. The GGM was in another concept constructed by 3 different types of wavelengths: long wavelength, medium wavelength and short wavelength. The long wavelength is used at orders and degrees of 0 to 360 and is characterized by being able to capture large-scale variations in the gravity field, such as broader topographic features. Meanwhile, the medium wavelength can capture medium-scale variations in the gravity field, such as more general topographic features. Then, the short wavelength can capture small-scale gravity fields, such as smaller topographic features.

Based on latest document on Implementation Roadmap of Vertical Reference System and Frame of Indonesia on the year 2020 to 2024, the accuracy of INAGEOID2020 needs to be further developed to reach the 5 cm requirement, especially to be able to robustly be used for large-scale mapping purpose. Many previous research has exactly tried to tackle this issue, with an emphasis on the ocean found that existing models has comparable accuracy (Zhang et al., 2021). Additionally, in Indonesia, several research has been conducted locally in specific island; Kalimantan (Hartanto et al., 2018), Sulawesi (Heliani & Noviantara, 2024), Bali (Udama et al., 2024) and Yogyakarta (Lestari et al., 2023). INAGEOID2020 v2.0 incorporates the EGM2008 global geopotential model (GGM) as its longwave component. Indeed, EGM2008 is a decades-old global model, with more recent models including XGM2019 and SGG-UGM-2. The two most recent models share the same maximum order and degree as the EGM2008 model, which is 2190. Hence, this work performed an assessment of the EGM2008, XGM2019e, and SGG-UGM-2 models employing order, degree, and truncation techniques that are appropriate for implementation in INAGEOID2020, similar to what have been done in other parts of the world; Sri Lanka (De Silva & Prasanna, 2023), Sudan (Godah & Krynski, 2015), Nigeria (Odumosu et al., 2021) and Turkey (Erol et al., 2009). Root Mean Square Error (RMSE) is utilized as a parameter to assess the robustness and accuracy of aforementioned GGMs. This research is expected to contribute on the fledging sub-field of validation and verification of existing models and data to update and develop regional and local geoid model further in the world, especially in Indonesia. Additionally, this research is expected to contribute to the fulfillment of the requirement outlined on the Technical Roadmap of Vertical Reference System and Reference in Indonesia.

Data and Method

The research was conducted in Balikpapan City - Samarinda City, East Kalimantan Province at the coordinates of 0° 12' S - 1° 30' S and 116° 24' E - 117° 42' E with an Area of Interest (AOI) of approximately 20,942 km^2,

as shown in **Figure 1**. The main reason this location is used as a research location is because one of the districts in East Kalimantan Province will be used as the new capital of the Republic of Indonesia named the Ibukota Nusantara (IKN) whose location coincides in the North Penajam Paser Regency area. IKN is also one of the national strategic projects listed in the 2020-2024 Rencana Pembangunan Jangka Menengah Nasional (RPJMN). In addition, the selection of this location is also because the geoid validation point in this area has been measured by the Badan Informasi Geospasial (BIG) from Balikpapan City to Samarinda City by passing through Kutai Kartanegara Regency.

There are four data used, including global geopotential models (GGMs) undulation data, INAGEOID2020 v2.0 data, tidal station data, and validation data. The GGM undulation data is used as the main data in this study which is downloaded at https://icgem.gfz-potsdam.de/. The GGM data consists of three kinds of models, namely EGM2008, XGM2019e, and SGG-UGM-2. Each model is performed at the maximum order and degree of 2190. then truncated at the order and degree of 720 and 360 and performed at the maximum order and degree of 720 and 360, listed on **Table 1**. In addition to GGM, INAGEOID2020 v2.0 data was also downloaded via https://srgi.big.go.id/geoid-active. These data were downloaded at a spatial resolution of 0.01° × 0.01°. The other data is the Tidal Station MSL data used as fitting data to be applied to the GGM. The MSL data used in this study uses the MSL value that was also used in the creation of INAGEOID2020 v2.0. This is so that the fitting done on the GGM is in line with the fitting done on INAGEOID2020 v2.0. In addition, there is validation data used as validation control to calculate the accuracy of the global geopotential model. The amount of validation data contained in East Kalimantan Province is 264 points spread as presented in Figure 1. The validation control points have been acquired by the Geospatial Information Agency using GNSS/Leveling method starting from Balikpapan Tidal Station through Kutai Kartanegara Regency to Samarinda City then back to Balikpapan Tidal Station. The measurement and acquisition results are in the form of information on the latitude, longitude, and geometric undulation values of each point.

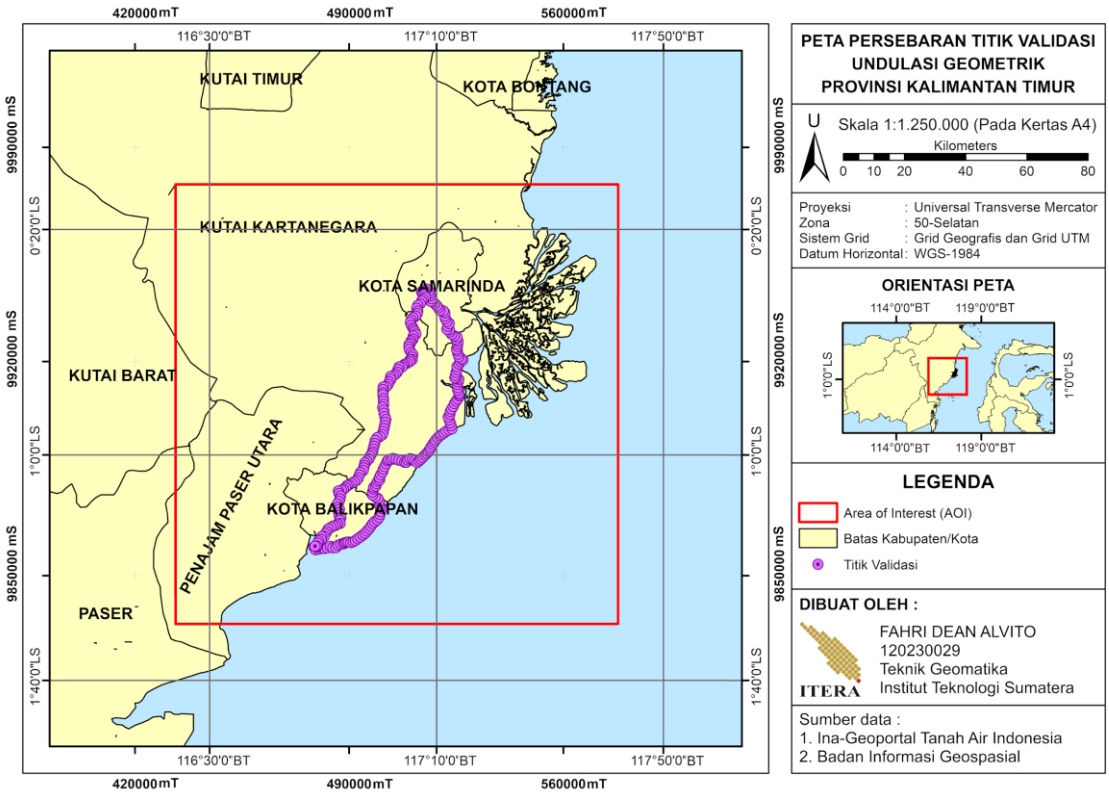

Figure 1. Research Location Map and Validation Points of East Kalimantan Province

Table 1. Global Geopotential Models (GGM) Samples

No.	Models	Max Degree	Truncation
1	EGM2008_2190	2190	-
2	EGM2008_2190_t_720	2190	720
3	EGM2008_2190_t_360	2190	360
4	EGM2008_720	720	-
5	EGM2008_360	360	-
6	XGM2019e_2190	2190	-
7	XGM2019e_2190_t_720	2190	720
8	XGM2019e_2190_t_360	2190	360
9	XGM2019e_720	720	-
10	XGM2019e_360	360	-
11	SGG-UGM-2_2190	2190	-
12	SGG-UGM-2_2190_t_720	2190	720
13	SGG-UGM-2_2190_t_360	2190	360
14	SGG-UGM-2_720	720	-
15	SGG-UGM-2_360	360	-

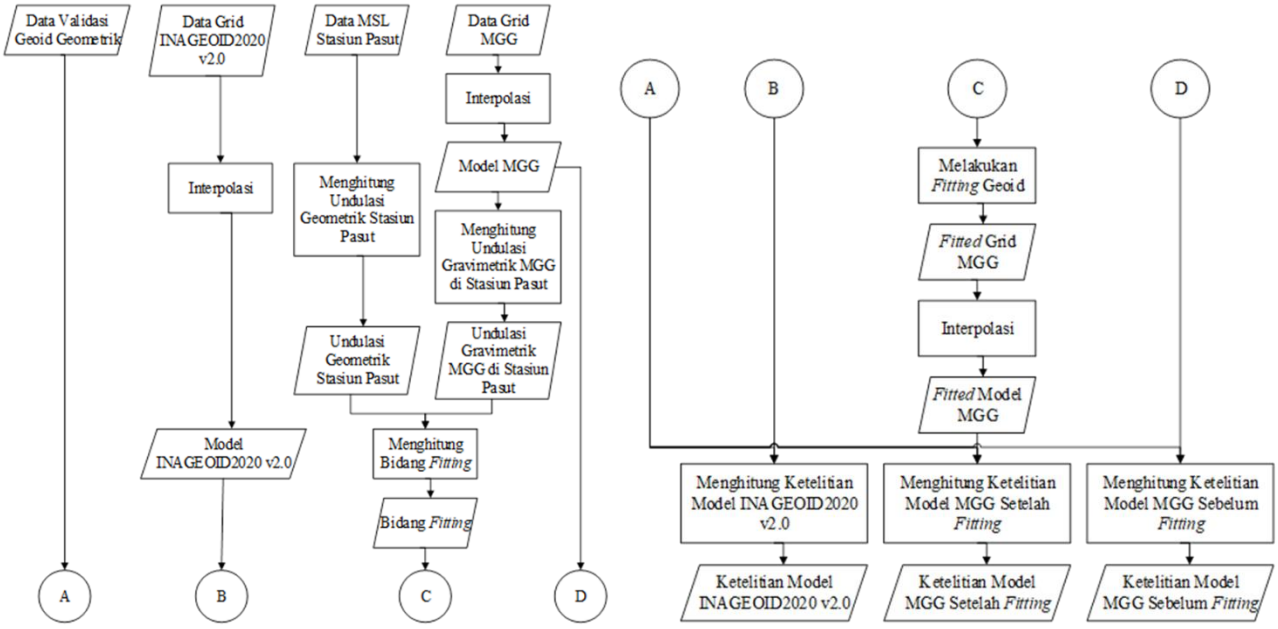

Figure 2. Research methodology flowchart

This research is divided by several steps and processes, which are shown in **Figure 2**. It started by obtaining the GGM with associated order and degree. The concepts of order and degree are determined based on mathematical functions defined on the surface of the sphere, namely Spherical Harmonics. In Spherical Harmonics, the determination of order and degree involves a mathematical equation referred to as the Laplace Equation and then defined in a spherical coordinate system (Müller, 1966). Harmonic potential is used to satisfy the Laplace Equation and is represented as Solid Spherical Harmonics. Solid Spherical Harmonics are used to represent potential inside a sphere. In practice, the potential inside the sphere is defined as the Earth's gravity field and is defined in terms of a spherical harmonic series, shown in **Equation 1** (Barthelmes, 2013). r, λ, φ is the spherical geocentric coordinate of the reference radius of the computing point (radius, longitude, latitude), *R* is the reference radius, *GM* is the gravitational constant and the mass of the earth, *l, m* is the degree and order of Spherical Harmonics, P_{lm} is the normalized Legendre function, dan C_{lm}^{W}, S_{lm}^{W} is the normalized Stokes coefficient.

$$W_a(r,\lambda,\varphi) = \frac{GM}{R}\sum_{l=0}^{l_{max}}\sum_{m=0}^{l}\left(\frac{R}{r}\right)^{l+1} P_{lm}(sin\ sin\ \varphi)(C_{lm}^{W}\ cos\ cos\ m\lambda\ + S_{lm}^{W}\ sin\ sin\ m\lambda) \quad (1)$$

The interpolation process is the initial stage of data processing after obtaining 15 GGM gravimetric undulation samples and INAGEOID2020 v2.0 gravimetric undulation data in the form of a 0.01° × 0.01° grid. The grid data were interpolated using spatial data processing software using the Kriging method. This method provides an estimate of the unobserved location of the variable Z, based on a weighted average of adjacent observed locations within a given area. The theory is derived from a regionalized variable and can be briefly explained by considering an intrinsic random function denoted by $Z(S_i)$, which represents all sample locations with i = 1, 2, ..., n. An estimate of the mean given by Kriging at unsampled $Z(S_0)$ locations is defined in **Equation 2** (Setianto & Triandini, 2015). $Z(S_i)$ is the measured value at the i-th location, λ_i is the unknown weight for the measured value at the i -th location, S_0 is the predicted location, and n is the number of measured values. The result of this interpolation produces a visualization of the geoid model, both visualizations on each sample of the GGM model and the INAGEOID2020 v2.0 model. From the visualization, the minimum, maximum, and average height values of the undulation of the geoid model can be known. In the GGMs processing, interpolation is done twice, namely on the GGMs grid before fitting is applied and on the GGMs grid after fitting is applied.

$$Z(S_0) = \sum_{i=1}^{n} \lambda_i Z(S_i) \tag{2}$$

Gravimetric undulation calculations were performed on all fifteen samples of the GGMs models. This calculation was carried out to obtain the value of the gravimetric undulation of the GGM at the tide station. The results of the interpolation on the GGMs were calculated by taking the gravimetric undulation value at the point of the tide station using spatial data processing software with the vectorization method, which is taking points from raster data into vectors. The results obtained are the GGMs gravimetric undulation values of each model sample at the tide station point. The gravimetric undulation value of each GGMs model sample will later be used as part of the calculation of the fitting field. Calculation of geometric undulation is performed to obtain the geometric undulation value at the tidal station point of Balikpapan city. This calculation is done by reducing the value of ellipsoid height (h_{ell}) with the value of mean sea level (H_{MSL}) of the tidal station. Then to get the geometric undulation, it is written in mathematical form in **Equation 3** (Torge et al., 2023). In determining the geometric undulation, the ellipsoid height value is obtained from the GNSS measurement results, and the MSL height is obtained from the tidal observation measurement results. This calculation produces a geometric undulation value (N_{geom}) at the tide station. The geometric undulation value of the tide station will later be used as the basis for the calculation of the fitting field.

$$N_{geom} = h_{ell} - H_{MSL} \tag{3}$$

The calculation of the fitting plane is done to produce a fitting plane that will be used to fit the geoid model. The calculation is done by setting aside the geometric undulation value of the tide station and the gravimetric undulation of each GGM at the tide station, as shown in **Equation 4**. N_{geom} is the geometric undulation at the tidal station and $N_{grav-MSL}$ is the GGM gravimetric undulation at the tidal station. This calculation was performed on all fifteen model samples. Each of these models will get a different fitting field value depending on the value of the gravimetric undulation at the tidal station of each model as shown in **Table 2**.

$$\Delta N = N_{geom} - N_{grav-MSL} \tag{4}$$

Geoid fitting is done to bring the gravimetric undulation value from GGMs closer to the geometric undulation from the tide station. The fitting method used in this study is the shifting method. This method reduces the model gravimetric undulation value (N_{grav}) by the fitting field value (ΔN) to produce the corresponding GGMs gravimetric undulation value against the geometric undulation, shown on **Equation 5**. After that, shifting is performed by summing the gravimetric undulations of the model geoid with a fitting field (ΔN).

$$N_{fitting} = N_{grav} + \Delta N \tag{5}$$

Table 2. Fitting Field

No	GGMs	N_{geom} (m)	$N_{grav\text{-}pasut}$ (m)	ΔN (m)
1	EGM2008_2190	53.376	52.964	0.412
2	EGM2008_720	53.376	52.960	0.416
3	EGM2008_360	53.376	53.128	0.248
4	EGM2008_2190_t_720	53.376	52.966	0.410
5	EGM2008_2190_t_360	53.376	52.967	0.409
6	XGM2019e_2190	53.376	52.904	0.472
7	XGM2019e_720	53.376	52.874	0.502
8	XGM2019e_360	53.376	53.025	0.351
9	XGM2019e_2190_t_720	53.376	52.905	0.471
10	XGM2019e_2190_t_360	53.376	52.904	0.472
11	SGG-UGM-2_2190	53.376	52.672	0.704
12	SGG-UGM-2_720	53.376	52.654	0.722
13	SGG-UGM-2_360	53.376	52.816	0.560
14	SGG-UGM-2_2190_t_720	53.376	52.666	0.710
15	SGG-UGM-2_2190_t_360	53.376	52.666	0.710

$N_{fitting}$ is the undulation after fitting, N_{grav} is the undulation before fitting the model and ΔN is the fitting field. The first step taken during the fitting process is that the results of the initial interpolation process in the form of visualization of the GGMs model are vectorized by converting raster data into grid-shaped vector data with a size of 0.01° × 0.01°. Data that has become a grid is calculated using number processing software. After that, the fitting process is carried out using the shifting method to produce data in the form of a fitted GGMs grid. The fitted data will be interpolated again to produce a visualization of the fitted GGMs model.

The calculation of geoid accuracy is part of the geoid model validation process. The calculation of geoid accuracy is carried out by calculating the difference between geometric undulations at 264 validation points and gravimetric undulations of the geoid model. The calculation is carried out on the INAGEOID2020 v2.0 model, the GGM models before fitting, and the GGM models after fitting. This calculation uses two parameters, namely Standard Deviation and Root Mean Square Error (RMSE). Standard deviation is calculated by squaring the distance of each value to its data center, the mean. Each squared distance is then averaged by summing the squared distances and then dividing by the amount of data minus one $(n-1)$, assuming that we are in the context of sample standard deviation as shown in **Equation 6**. σ is the standard deviation, ΔN_i is the difference in undulations between gravimetric undulations and geometric undulations, $\Delta\underline{N_i}$ is the mean of ΔN_i, and n is the amount of data. Standard deviation is used to measure the spread of data of a numerical variable. The larger the standard deviation value, the more diverse or spread out the data is from the mean value.

$$\sigma = \sqrt{\frac{\sum_i^n (\Delta N_i - \Delta\underline{N_i})^2}{(n-1)}} \tag{6}$$

RMSE is calculated by squaring the error (the difference between the predicted value and the actual value), then finding the average by summing the squared error and then dividing by the amount of data (n). Mathematically, it can be written as **Equation 7**. where N_{geom} is the geometric undulation, Ngrav is the gravimetric undulation, and n is the amount of data. RMSE is used to measure the error rate of a model in predicting a numerical value. The smaller the RMSE value, the more accurate the model is in predicting. RMSE is the number of areas divided by the number of actual values. Note that if we use the mean value as the predicted value, the RMSE value will be equal to the standard deviation value. This shows the relationship between RMSE and standard deviation.

$$RMSE = \sqrt{\frac{\sum_i^n \left(N_{geom} - N_{grav}\right)^2}{n}} \tag{7}$$

Results and Discussion

The INAGEOID2020 v2.0 model and Global Geopotential Models (GGMs) were used to create a geoid model visualization, shown in **Figure 3**. INAGEOID2020 v2.0 displayed the highest undulation value compared to other GGMs, with a height range of 52.50 m to 53.00 m and a very intense hue. It also had a pronounced orange hue in the eastern district of Samarinda City. The production process of INAGEOID2020 v2.0 involved using tide stations benchmarks around Indonesia for fitting purposes, resulting in a larger undulation value in INAGEOID2020 v2.0 compared to the GGMs reference. In the southwest region of Balikpapan City, SGG-UGM-2 displayed a broader blue hue compared to EGM2008 and XGM2019e, indicating that the geoid plane on SGG-UGM-2 is slightly lower compared to other two GGM, skewed on the southwest direction since in the other direction the hues on all three GGMs are similar. Differences may arise due to variations in the input data elements of each global model, especially the satellite gravity and terrestrial and airborne gravity. Refinement of the Earth's mass distribution by gravity satellites like GRACE and GOCE directly affects the magnitude of geoidal undulations (Liang et al., 2020; Pail, 2014). Terrestrial and airborne gravity measurements enhance the accuracy of local gravity fluctuations, particularly in land regions with intricate topography (Jiang et al., 2020; Pavlis et al., 2012).

Further analysis on truncation effect on the GGMs is visualized in **Figure 4**. The visual representation in Figure 4 illustrates the variations in the identification of the limits of order, degree, and truncation of the model proposed in EGM2008 as one of the examples. The disparity in model representation arises from the spatial resolution generated by each model. The level and complexity of a model directly correlate with the level of detail captured about the Earth's gravity field, which in turn generates undulations in the geoid model. According to research by Hartanto & Chabibi in 2019, the order and degree of 2190 increase the detail in representing topographic conditions due to the high spectral resolution so that it can capture short-wavelengths with small details of the Earth's gravity field. Models with higher degree and order can also capture shorter full-wavelengths, thus providing more detailed information about the gravity field. Full-wavelength refers to the full wavelength that a particular gravity model can capture. This relates to the ability of the model to capture variations in the gravity field over a wide range of scales, from very large to very small. The EGM2008 model with an order and degree of 720 and 360 (Figure 4(d) and (e)) has a lower resolution than the model with an order and degree of 2190 which results in a different contour pattern compared to the order and degree of 2190. Models with lower degrees and orders, such as 720 and 360, are more sensitive to long-wavelength and medium-wavelength, resulting in visualizations that are smoother and less detailed than higher orders and degrees in capturing smaller variations in the gravity field. The EGM2008 model with a maximum degree and order of 2190 which is truncated at 720 and 360 degrees (Figure 4(b) and (c)) also influences the detail of the model resulting in different contour patterns in the truncated model, especially on the 360. This is because truncation acts as low-pass filtering in the frequency domain to retain low-frequency components and ignore high-frequency components to simplify the model (Barthelmes, 2013) This truncation acts as a filter to remove noise or unwanted signals that may be present at very high levels of detail, thus helping to improve the quality of relevant data and reduce unnecessary noise.

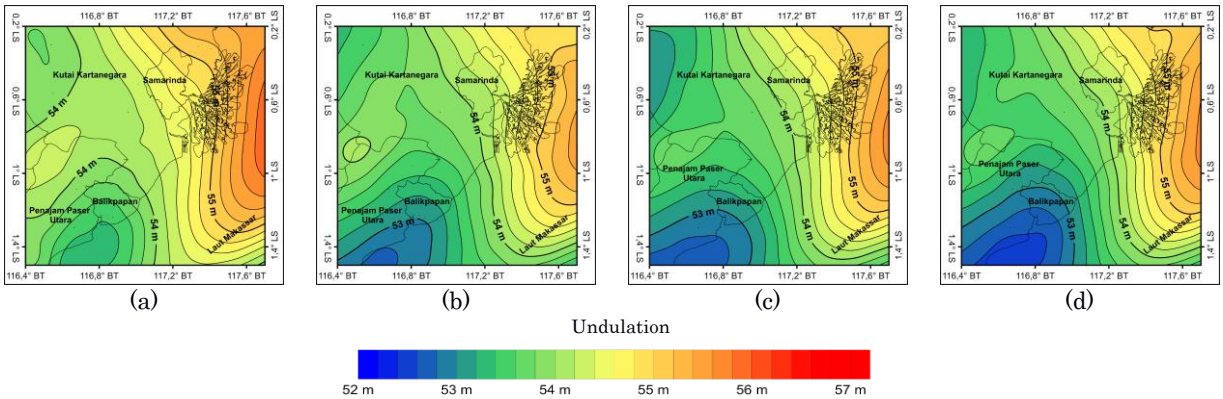

Figure 3. Model Visualization of (a) INAGEOID2020 v2.0; and GGM (b) EGM2008 degrees 2190, (c) XGM2019e degrees 2190, and (d) SGG-UGM-2 degrees 2190

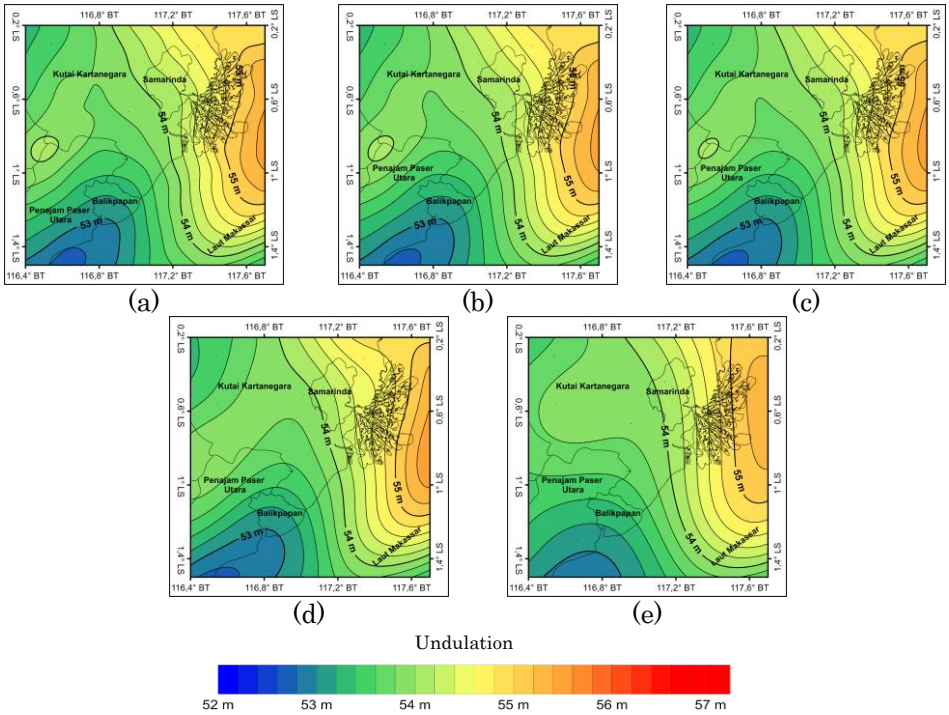

Figure 4. Model Visualization (a) EGM2008_2190, (b) EGM2008_2190_t_720, (c) EGM2008_2190_t_360, (d) EGM2008_720, and (e) EGM2008_360

Geoid fitting affects the undulation value on GGMs, which makes the undulation of GGMs after fitting almost the same value as the INAGEOID2020 v2.0 model. The value of the difference between before and after fitting depends on the value of the fitting field in each model, which is in the range of 0.248 m - 0.723 m as shown in Table 2. This is because the fitting is done with the same value in the entire study area based on the fitting field in each model. In the graph, EGM2008 and XGM2019e after the fitting process produce averages similar to INAGEOID2020 v2.0. Meanwhile, in SGG-UGM-2 after fitting, the average value is greater than the undulation value of INAGEOID2020 v2.0, shown as higher dark green line in Figure 5. This can also be seen in the graph of its gravimetric undulations against the geometric undulations at each validation point presented in **Figure 5**. Before fitting, the height values of SGG-UGM-2 in this range were lower than those of EGM2008 and XGM2019e. It can be seen in Figure 5(b) that the GGM undulations have a better fit to the geometric undulations, especially the EGM2008 and XGM2019e models. Figure 5(b) also shows that both models fit the INAGEOID2020 v2.0 undulations and geometric undulations quite well. However, in SGG-UGM-2, the undulations in the middle range of the graph are higher than the geometric undulations. This can happen because the fitting is done at the tide station point located at point 1 or point 265 on the graph. Therefore, when before fitting there is a difference in undulation in the early and late ranges, then after fitting there is a difference in the middle range. This makes the SGG-UGM-2 model less suitable for INAGEOID2020 v2.0 undulations and geometric undulations. The calculation of GGM accuracy is used as the basis for evaluating the use of GGM in the INAGEOID2020 v2.0 model. The calculation of GGM accuracy was carried out on three GGM models, namely EGM2008, XGM2019e, and SGG-UGM-2. Of the three models, restrictions were made based on the maximum degree order of 2190, 720, and 360. In addition, the calculation is also truncated applied to the order and degree of 360 and 720, all shown in **Table 3**.

Table 3. GGM Accuracy Value Before Fitting

No	GGMs	Min (m)	Max (m)	Avg (m)	St. Dev (m)	RMSE (m)
1	EGM2008_2190	0.229	0.640	0.454	0.071	0.460
2	EGM2008_2190_t_720	0.226	0.636	0.454	0.069	0.459
3	EGM2008_2190_t_360	0.224	0.636	0.454	0.068	0.459
4	EGM2008_720	0.230	0.627	0.448	0.069	0.453
5	EGM2008_360	0.059	0.649	0.369	0.088	0.380

No	GGMs	Min (m)	Max (m)	Avg (m)	St. Dev (m)	RMSE (m)
6	XGM2019e_2190	0.282	0.644	0.450	0.063	0.454
7	XGM2019e_2190_t_720	0.281	0.643	0.451	0.061	0.455
8	XGM2019e_2190_t_360	0.282	0.645	0.452	0.061	0.456
9	XGM2019e_720	0.287	0.675	0.457	0.068	0.462
10	XGM2019e_360	0.160	0.700	0.423	0.078	0.430
11	SGG-UGM-2_2190	0.363	0.891	0.613	0.121	0.624
12	SGG-UGM-2_2190_t_720	0.364	0.890	0.613	0.118	0.624
13	SGG-UGM-2_2190_t_360	0.367	0.887	0.613	0.118	0.624
14	SGG-UGM-2_720	0.339	0.895	0.606	0.126	0.619
15	SGG-UGM-2_360	0.342	0.738	0.535	0.070	0.540

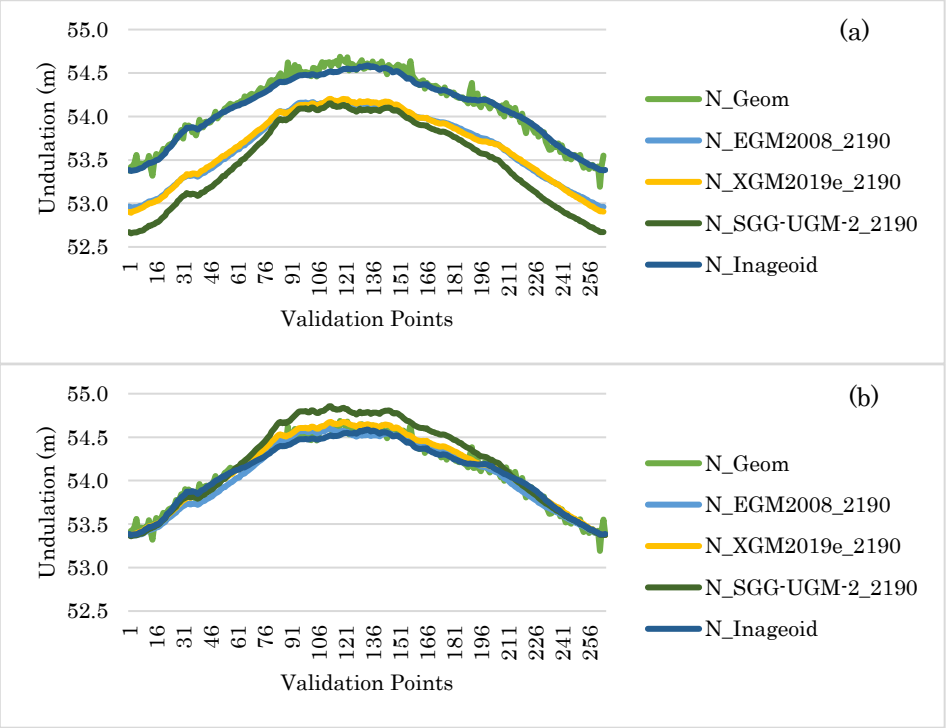

Figure 5. Graph of INAGEOID2020 v2.0 Undulation and GGM degree 2190 Undulation against Geometric Undulation (a) Before Fitting, and (b) After Fitting

Based on the results of the accuracy calculation presented in Table 3, the models that have the highest accuracy value based on standard deviation (STD) are XGM2019e_2190_t_720 and XGM2019e_2190_t_360 with a value of 0.061 m, and the model that has the highest accuracy value based on RMSE is EGM2008_360 with a value of 0.380m. This means that the XGM2019e_2190_t_720 and XGM2019e_2190_t_360 models are the most precise but less accurate models of geometric undulations based on the validation points. All models have RMSE values that are much larger than STD. This is because the GGM does not fit the geometric undulations. This means that the models are quite precise to the geometric undulations but not accurate on the validation points provided. Especially for the SGG-UGM-2 model, the RMSE value is larger than the EGM2008 and XGM2019e models. This is influenced by the difference in undulation values between the initial and final validation points that are located on the coast, making the RMSE value of the model larger. This indicates that SGG-UGM-2 has a slight problem on the transition between land and ocean compared to other two GGM. This could also be a culprit in the usage of different coastal data on these three models. Therefore, the fitting process is carried out so that the GGM gravimetric undulations are fit to the geometric undulations. When the models have not been fitted, the three GGM geoid models show geoid RMSE values ranging from 0.370 m - 0.620 m. This value is very different from the RMSE in INAGEOID2020 v2.0. Therefore, GGM was fitted to improve the RMSE value, with results listed in **Table 4**.

Table 4. GGM Accuracy Value After Fitting

No	GGMs	Min (m)	Max (m)	Avg (m)	St. Dev (m)	RMSE (m)
1	EGM2008_2190	-0.183	0.228	0.042	0.071	0.082
2	EGM2008_2190_t_720	-0.184	0.225	0.044	0.069	0.081
3	EGM2008_2190_t_360	-0.185	0.226	0.045	0.068	0.081
4	EGM2008_720	-0.187	0.210	0.032	0.069	0.076
5	EGM2008_360	-0.189	0.401	0.121	0.088	0.150
6	XGM2019e_2190	-0.191	0.172	-0.022	0.063	0.066
7	XGM2019e_2190_t_720	-0.190	0.172	-0.020	0.061	0.064
8	XGM2019e_2190_t_360	-0.191	0.172	-0.020	0.061	0.064
9	XGM2019e_720	-0.216	0.172	-0.046	0.068	0.082
10	XGM2019e_360	-0.191	0.349	0.072	0.078	0.106
11	SGG-UGM-2_2190	-0.342	0.186	-0.092	0.121	0.152
12	SGG-UGM-2_2190_t_720	-0.346	0.179	-0.097	0.118	0.153
13	SGG-UGM-2_2190_t_360	-0.343	0.177	-0.098	0.118	0.153
14	SGG-UGM-2_720	-0.383	0.173	-0.116	0.126	0.172
15	SGG-UGM-2_360	-0.219	0.177	-0.025	0.070	0.074

As shown in Table 4, the accuracy of GGM based on RMSE increased after the fitting process, but the STD remained. The results in this study are different from the research conducted by (Pahlevi et al., 2024), which showed that the accuracy based on STD after the fitting process also increased. This difference can occur because in previous research, the fitting field data used is tide stations benchmark spread throughout Indonesia. The fitting field is interpolated to produce different fitting field values in each region. Because of this difference, the STD before and after fitting can change. STD is calculated based on the square between the difference of gravimetric and geometric undulations to their mean value and when fitting is done with different fitting field values, the mean value in the fitted model will also be different. Meanwhile, the fitting field data used in this study only uses tide station benchmark in Balikpapan. Therefore, the STD in this study is fixed due to the same value of the fitting field. Furthermore, the XGM2019e_2190_t_720 and XGM2019e_2190_t_360 models have the highest accuracy value with an accuracy value based on STD of 0.061 m and based on RMSE of 0.064 m, which means that the model has a high level of precision and accuracy compared to other GGM models. While the SGG-UGM-2_720 model gets the lowest accuracy value with an accuracy value based on STD of 0.126 m and based on RMSE of 0.172 m, which means that the model has a low level of precision and accuracy compared to other models. However, all these models still do not meet the expected accuracy target in the Indonesian region, which is 5 cm. Therefore, it is necessary to do geoid modeling on each GGM using a combination of free-air gravity data and topographic correction to produce a more accurate geoid model. This is because in geoid modeling, the GGM acts as a long-wave component, free-air gravity acts as a medium-wave component, and topographic data acts as a short-wave component (Pahlevi et al., 2019). In terms of truncation results, Table 4 provides information that truncation will slightly increase the precision value of a model but will not necessarily increase the accuracy of the model. This is evidenced by the increase in the accuracy values of EGM2008 and XGM2019e after truncation is applied to the order and degree of 720 and 360. This means that the noise contained in the model with order and degree 2190 has been removed, resulting in a more precise model. In this case, XGM2019e_2190_t_720 and XGM2019e_2190_t_360 are the most accurate models in representing medium or short waves that reflect features with large spatial resolution.

Conclusions

Before fitting, the GGM model did not fit the INAGEOID2020 v2.0 undulations and geometric undulations. After fitting, the fitting levels improved although the fitting field values were different among the tested models. Fitting was performed on the Balikpapan tide station benchmark with a value range of 0.248 m - 0.560. Among the models fitted, only EGM2008 and XGM2019e have better fits to the INAGEOID2020 v2.0 undulations and geometric undulations. In contrast, SGG-UGM-2 was not fit due to the difference in elevation

values at the beginning and end of the validation point used as the fitting plane, causing a mismatch with the INAGEOID2020 v2.0 undulations and geometric undulations.

Evaluation of the use of a global geopotential model as an alternative component of INAGEOID2020 v2.0, namely by using the XGM2019e_2190 model which is truncated 720 and 360 can be considered as a replacement for EGM2008 for the next INAGEOID2020 generation component, because the model gets the highest accuracy in STD and RMSE of 0.061 m and 0.064 m after the fitting process. In addition, another model to consider is the 360-degree SGG-UGM-2 which produces higher STD and RMSE values of 0.070 m and 0.074 m, respectively, which is a suitable model for representing data at long waves. However, the visualizations and graphs produced by SGG-UGM-2 look very different from those presented in EGM2008 and XGM2019e. In addition, the accuracy value of SGG-UGM-2 at orders and degrees other than 360 is very low compared to EGM2008 and XGM2019e. Therefore, XGM2019e is suggested to be utilized as a substitute for EGM2008 in the next iteration of INAGEOID2020.

Further research needs to be done by applying Gaussian Filters to each GGM to produce a more accurate geoid model. In addition, in terms of modeling geoid, GGM data needs to be combined with free-air gravity data and topographic correction to produce a more accurate geoid model. The distribution of GNSS/Levelling measurement points in the form of geometric undulation values to perform validation calculations on the gravimetric undulation model also needs to be more widely measured to represent every region in East Kalimantan Province. Finally, it is necessary to do geoid fitting with tide stations throughout Indonesia so that the fitting results become more in line with geometric undulations.

References

Andersen, O. B., & Knudsen, P. (2019). The DTU17 Global Marine Gravity Field: First Validation Results. In S. P. Mertikas & R. Pail (Eds.), *Fiducial Reference Measurements for Altimetry* (Vol. 150, pp. 83–87). Springer International Publishing. https://doi.org/10.1007/1345_2019_65

Barthelmes, F. (2013). Definition of functionals of the geopotential and their calculation from spherical harmonic models: Theory and formulas used by the calculation service of the International Centre for Global Earth Models (ICGEM); http://icgem.gfz-potsdam.de/ICGEM/ ; revised edition. *Scientific Technical Report; 09/02; ISSN 1610-0956*. https://doi.org/10.2312/GFZ.B103-0902-26

Bramanto, B., Prijatna, K., Fathulhuda, M. S., & Pahlevi, A. M. (2022). Gravimetric Geoid Modeling by Stokes and Second Helmert's Condensation Method in Yogyakarta, Indonesia. In J. T. Freymueller & L. Sánchez (Eds.), *Geodesy for a Sustainable Earth* (Vol. 154, pp. 147–153). Springer International Publishing. https://doi.org/10.1007/1345_2022_149

De Silva, W. J. P., & Prasanna, H. M. I. (2023). Comparison of different global DTMs and GGMs over Sri Lanka. *Journal of Applied Geodesy*, *17*(1), 29–38. https://doi.org/10.1515/jag-2022-0026

Erol, B., Sideris, M. G., & Çelik, R. N. (2009). Comparison of global geopotential models from the champ and grace missions for regional geoid modelling in Turkey. *Studia Geophysica et Geodaetica*, *53*(4), 419–441. https://doi.org/10.1007/s11200-009-0032-8

Featherstone, W. E., Filmer, M. S., Claessens, S. J., Kuhn, M., Hirt, C., & Kirby, J. F. (2012). Regional geoid-model-based vertical datums – some Australian perspectives. *Journal of Geodetic Science*, *2*(4), 370–376. https://doi.org/10.2478/v10156-012-0006-6

Feng, W., Zhong, M., & Xu, H. (2012). Sea level variations in the South China Sea inferred from satellite gravity, altimetry, and oceanographic data. *Science China Earth Sciences*, *55*(10), 1696–1701. https://doi.org/10.1007/s11430-012-4394-3

Förste, C., Bruinsma, Sean. L., Abrikosov, O., Lemoine, J.-M., Marty, J. C., Flechtner, F., Balmino, G., Barthelmes, F., & Biancale, R. (2014). *EIGEN-6C4 The latest combined global gravity field model including GOCE data up to degree and order 2190 of GFZ Potsdam and GRGS Toulouse* (p. 55102156 Bytes, 3 Files) [Application/octet-stream,application/octet-stream,application/zip]. GFZ Data Services. https://doi.org/10.5880/ICGEM.2015.1

Godah, W., & Krynski, J. (2015). Comparison of GGMs based on one year GOCE observations with the EGM08 and terrestrial data over the area of Sudan. *International Journal of Applied Earth Observation and Geoinformation*, *35*, 128–135. https://doi.org/10.1016/j.jag.2013.11.003

Goyal, R., Featherstone, W. E., Claessens, S. J., Dikshit, O., & Balasubramanian, N. (2021). *The Indian gravimetric geoid model based on the Stokes-Helmert approach with Vaníček-Kleusberg modification of the Stokes kernel: IndGG-SH2021* (Version 1.0) [Dataset]. GFZ Data Services. https://doi.org/10.5880/ISG.2021.009

Hartanto, P., & Chabibi, F. F. (2019). UJI KETELITIAN MODEL GEOPOTENSIAL GLOBAL DI PULAU JAWA DAN MADURA. *Seminar Nasional Geomatika*, *3*, 827. https://doi.org/10.24895/SNG.2018.3-0.1071

Hartanto, P., Huda, S., Putra, W., Variandy, E. D., Triarahmadhana, B., Pangastuti, D., Pahlevi, A. M., & Hwang, C. (2018). Estimation of marine gravity anomaly model from satellite altimetry data (Case Study: Kalimantan and Sulawesi Waters-Indonesia). *IOP Conference Series: Earth and Environmental Science*, *162*, 012038. https://doi.org/10.1088/1755-1315/162/1/012038

Heliani, L. S., & Noviantara, H. (2024). Pengaruh Densitas Topografi Terhadap Ketelitian Model Geoid: Studi kasus Pulau Sulawesi. *JGISE: Journal of Geospatial Information Science and Engineering*, *7*(2), 191. https://doi.org/10.22146/jgise.102122

Hofmann-Wellenhof, B., Lichtenegger, H., & Wasle, E. (2008). *GNSS — Global Navigation Satellite Systems*. Springer Vienna. https://doi.org/10.1007/978-3-211-73017-1

Hofmann-Wellenhof, B., & Moritz, H. (2006). *Physical Geodesy*. Springer Vienna. https://doi.org/10.1007/978-3-211-33545-1

Jiang, T., Dang, Y., & Zhang, C. (2020). Gravimetric geoid modeling from the combination of satellite gravity model, terrestrial and airborne gravity data: A case study in the mountainous area, Colorado. *Earth, Planets and Space*, *72*(1), 189. https://doi.org/10.1186/s40623-020-01287-y

Kahar, J. (1982). Geoid Determination in Archipelago Area. *Processing of General Meeting of AIG*, 466–471.

Kahar, J., Kasenda, A., & Prijatna, K. (1996). *The Indonesian Geoid Model 1996*. 613–620.

Lestari, R., Bramanto, B., Prijatna, K., Pahlevi, A. M., Putra, W., Muntaha, R. I. S., & Ladivanov, F. (2023). Local geoid modeling in the central part of Java, Indonesia, using terrestrial-based gravity observations. *Geodesy and Geodynamics*, *14*(3), 231–243. https://doi.org/10.1016/j.geog.2022.11.007

Liang, W., Li, J., Xu, X., Zhang, S., & Zhao, Y. (2020). A High-Resolution Earth's Gravity Field Model SGG-UGM-2 from GOCE, GRACE, Satellite Altimetry, and EGM2008. *Engineering*, *6*(8), 860–878. https://doi.org/10.1016/j.eng.2020.05.008

Müller, C. (1966). *Spherical Harmonics*. Springer Berlin / Heidelberg.

Nadzir, Z. A., & Rahmadhani, N. (2024). EVALUASI DAN KOMPARASI DARI MODEL ANOMALI GAYA BERAT di LAUTAN INDONESIA. *Jurnal Sains Informasi Geografi*, *7*(2), 99. https://doi.org/10.31314/jsig.v7i2.3073

Odumosu, J. O., Nnam, V. C., & Nwadialor, I. J. (2021). An assessment of spatial methods for merging terrestrial with GGM-derived gravity anomaly data. *Journal of African Earth Sciences*, *179*, 104202. https://doi.org/10.1016/j.jafrearsci.2021.104202

Pahlevi, A., Bramanto, B., Triarahmadhana, B., Huda, S., Pangastuti, D., Nur, A., Wijaya, D. D., Prijatna, K., Julianto, M., & Wijanarto, A. B. (2019). Airborne gravity survey, towards a precise Indonesian geoid model (case study: Sumatera Island). *IOP Conference Series: Earth and Environmental Science*, *389*(1), 012050. https://doi.org/10.1088/1755-1315/389/1/012050

Pahlevi, A., Syafarianty, A., Susilo, S., Lumban-Gaol, Y., Putra, W., Triarahmadhana, B., Bramanto, B., Muntaha, R., El Fadhila, K., Ladivanov, F., Amrossalma, H., Islam, L., Novianto, D., Huda, S., Wismadi, T., Efendi, J., Ramadhan, A., Wijaya, D., Prijatna, K., & Pramono, G. (2024). Geoid Undulation Model as Vertical Reference in Indonesia. *Scientific Data*, *11*(1), 822. https://doi.org/10.1038/s41597-024-03646-w

Pail, R. (2014). CHAMP-, GRACE-, GOCE-Satellite Projects. In E. Grafarend (Ed.), *Encyclopedia of Geodesy* (pp. 1–11). Springer International Publishing. https://doi.org/10.1007/978-3-319-02370-0_29-1

Pavlis, N. K., Holmes, S. A., Kenyon, S. C., & Factor, J. K. (2012). The development and evaluation of the Earth Gravitational Model 2008 (EGM2008). *Journal of Geophysical Research: Solid Earth*, *117*(B4), 2011JB008916. https://doi.org/10.1029/2011JB008916

Sabri, L. M., Sudarsono, B., & Pahlevi, A. (2021). Geoid of South East Sulawesi from airborne gravity using Hotine approach. *IOP Conference Series: Earth and Environmental Science*, *731*(1), 012014. https://doi.org/10.1088/1755-1315/731/1/012014

Sansò, F., & Sideris, M. G. (2013). *Geoid determination: Theory and methods*. Springer.
Seeber, G. (2003). *Satellite geodesy* (2nd completely rev. and extended ed). Walter de Gruyter.
Setianto, A., & Triandini, T. (2015). COMPARISON OF KRIGING AND INVERSE DISTANCE WEIGHTED (IDW) INTERPOLATION METHODS IN LINEAMENT EXTRACTION AND ANALYSIS. *Journal of Applied Geology*, *5*(1). https://doi.org/10.22146/jag.7204
Torge, W., Müller, J., & Pail, R. (2023). *Geodesy*. De Gruyter. https://doi.org/10.1515/9783110723304
Udama, Z. A., Claessens, S., Anjasmara, I. M., & Syafarianty, A. N. (2024). Analysis of different combinations of gravity data types in gravimetric geoid determination over Bali. *Journal of Applied Geodesy*, *18*(3). https://doi.org/10.1515/jag-2023-0042
Vaníček, P., & Krakiwsky, E. J. (1995). *Geodesy: The concepts* (2. ed., 5. print). Elsevier.
Zhang, S., Abulaitijiang, A., Andersen, O. B., Sandwell, D. T., & Beale, J. R. (2021). Comparison and evaluation of high-resolution marine gravity recovery via sea surface heights or sea surface slopes. *Journal of Geodesy*, *95*(6), 66. https://doi.org/10.1007/s00190-021-01506-8
Zingerle, P., Pail, R., Gruber, T., & Oikonomidou, X. (2020). The combined global gravity field model XGM2019e. *Journal of Geodesy*, *94*(7), 66. https://doi.org/10.1007/s00190-020-01398-0